

## Proton $h_{11/2}^2$ and Octupole Excitations in $^{148}\text{Dy}_{82}$ and $^{149}\text{Dy}_{83}$

P.J. Daly\*

Institut für Kernphysik, Kernforschungsanlage Jülich, Jülich, F.R. Germany  
and Chemistry Department, Purdue University, W. Lafayette, Indiana, USA

P. Kleinheinz, R. Broda\*\* and S. Lunardi\*\*\*

Institut für Kernphysik, Kernforschungsanlage Jülich, Jülich,  
Federal Republic of Germany

H. Backe

Institut für Kernphysik der TH Darmstadt, Darmstadt, Federal Republic of Germany

J. Blomqvist

Research Institute of Physics, Stockholm, Sweden

Received July 25, 1980

The yrast states of  $^{148}\text{Dy}$  and  $^{149}\text{Dy}$  have been studied by  $\gamma$ -ray and conversion electron measurements in  $(\alpha, xn)$  and  $(^{16}\text{O}, xn)$  reactions on enriched  $^{152}\text{Gd}$  and  $^{136}\text{Ce}$  targets. Level schemes to above 4 MeV for the two nuclei are reported. The  $\pi h_{11/2}^2$  spectrum identified in  $^{148}\text{Dy}$  and the  $\pi h_{11/2}$  effective charge  $e_{\text{eff}} = 1.52 \pm 0.05e$ , derived from the measured  $E2$  transition rate between the  $(\pi h_{11/2}^2) 10^+$  and  $8^+$  states, are discussed and compared with results for other two-particle nuclei. The yrast cascades in  $^{148}\text{Dy}$  and  $^{149}\text{Dy}$  continue above the  $(\pi h_{11/2}^2) 10^+$  and  $(\pi h_{11/2}^2 \nu f_{7/2}) 27/2^-$  states by  $\sim 1$  MeV  $E1$  transitions de-exciting the lowest members of octupole multiplets built on these states. The energy shifts for the observed members of the  $\pi h_{11/2}^2 \times 3^-$  multiplet are analyzed in terms of twoparticle-phonon exchange coupling using an empirical coupling strength extracted from the one valence particle nucleus  $^{147}\text{Tb}$ . The dominant  $\nu f_{7/2} \times 3^-$  character of low-lying  $13/2^+$  isomers in  $^{149}\text{Dy}$  and other  $N=83$  nuclei is emphasized.

### 1. Introduction

A recent analysis [1] of high-spin particle-hole excitations in the  $N=82$  nucleus  $^{146}\text{Gd}$  has shown that there is a large gap in the single particle spectrum at  $Z=64$ . We are examining the consequences of this gap by studying the nuclei around  $^{146}\text{Gd}$  to determine whether their high-spin level spectra can be described as successfully in shell model terms as those of the few valence particle nuclei around  $^{208}\text{Pb}$ . Studies of the one-particle nuclei  $^{147}\text{Gd}$  and  $^{147}\text{Tb}$  have already shown [1, 2] that their yrast states up to  $\sim 4$  MeV excitation energy arise from the coupling of the valence particle to the  $^{146}\text{Gd}$  core states, and recent results [3–5] for the one-hole nuclei  $^{145}\text{Gd}$

and  $^{145}\text{Eu}$  may also be interpreted in a similar way. An earlier investigation [6, 7] of the three valence particle nucleus  $^{149}\text{Dy}$  located a  $27/2^-$  isomeric state of  $\pi h_{11/2}^2 \nu f_{7/2}$  character and partially characterized the states populated in its decay to the  $^{149}\text{Dy} \nu f_{7/2}$  ground state.

We have now investigated the two-proton nucleus  $^{148}\text{Dy}$ , and have also obtained some useful new data for the  $^{149}\text{Dy}$  nucleus. Since the  $h_{11/2}$ ,  $s_{1/2}$  and  $d_{3/2}$  proton orbitals lie close together and are the only orbitals between the  $Z=64$  and  $Z=82$  gaps, one could anticipate that excitations involving  $h_{11/2}$  protons would be yrast states in the Dy nuclei. Specifically one could hope to observe in  $^{148}\text{Dy}$  a complete  $\pi h_{11/2}^2$  spectrum, similar to the well-studied [8]  $\pi h_{9/2}^2$  sequence in  $^{210}\text{Po}$ . In a short note [9], we have

\* Supported in part by the U.S. Department of Energy

\*\* Present address: Institute of Nuclear Physics, Cracow, Poland

\*\*\* Present address: I.N.F.N. Sezione di Padova, Padova, Italy

already summarized some of the results of the present investigation, including the identification of all the  $^{148}\text{Dy}$   $\pi h_{11/2}^2$  states.

The  $10^+$  coupling of the two  $h_{11/2}$  protons, which generates ten units of angular momentum at low cost in excitation energy, should play a particularly important role in the yrast spectroscopy of the Dy nuclei. The maximally aligned  $(\pi h_{11/2}^2)10^+$  and  $(\pi h_{11/2}^2 \nu f_{7/2})27/2^-$  states in  $^{148}\text{Dy}$  and  $^{149}\text{Dy}$  should have exceptionally pure configurations; however the energies of these states cannot be calculated from empirical single particle energies and nucleon-nucleon interactions because the ground state masses of the two nuclei are not known. Instead, as we show in a forthcoming paper [10], the experimental energies of these  $10^+$  and  $27/2^-$  states can be combined with spectroscopic information from neighbouring nuclei to yield rather precise estimates of the previously unknown ground state masses of  $^{148}, ^{149}\text{Dy}$  and several other nuclei in this region.

At  $I=10$ , the valence spin of  $^{148}\text{Dy}$  is exhausted, and it is not obvious a priori how the yrast line should continue above the  $(h_{11/2}^2)10^+$  state. The present investigation demonstrates that the next higher yrast states are of the type  $\pi h_{11/2}^2 \times 3^-$ , obtained by excitation of the low-lying  $^{146}\text{Gd}$   $3^-$  core state. Since the dominant component of that octupole excitation is  $\pi h_{11/2}^2 d_{5/2}^{-1}$ , we observe in  $^{148}\text{Dy}$  (and also in  $^{149}\text{Dy}$ ) novel and interesting features of two particle phonon exchange coupling.

## 2. Measurements and Results

### 2.1. The $^{148}\text{Dy}$ Level Scheme

At the start of this investigation, all that was known [11, 12] about  $^{148}\text{Dy}$  was that its 3.1 min  $\beta$ -decay populates exclusively a  $1^+$  level in  $^{148}\text{Tb}$  which de-excites by means of a 620 keV  $E1$  transition. Extensive excitation function measurements involving 70–100 MeV  $\alpha$ -particle bombardments of a  $\geq 99\%$  enriched  $^{152}\text{Gd}$  target and preliminary  $\gamma\gamma$  coincidence studies identified a cascade of 86, 94, 390, 661 and 1,688 keV  $\gamma$ -rays, which were assigned to  $^{148}\text{Dy}$  because they followed the same  $(\alpha, 8n)$  excitation function and had nearly the same intensity as the 620 keV  $\gamma$ -ray from the decay of  $^{148}\text{Dy}$ . The angular distributions of the five  $\gamma$ -rays were later found to be isotropic, and a lifetime measurement using a  $\mu\text{s}$  beam pulsing system showed that these transitions (and some other weaker ones) follow an isomer with a half life of about 0.5  $\mu\text{s}$ .

Comprehensive  $\gamma\gamma$  coincidence experiments were performed with two 70 cm<sup>3</sup> coaxial Ge(Li) detectors

using a pulsed beam of 106 MeV  $\alpha$ -particles on the  $^{152}\text{Gd}$  target; the interval between beam bursts on target was 120 ns. Coincidence data were stored in a four parameter  $(E_1, E_2, t_{12}, t_{2RF})$  mode and were later sorted by setting various energy gates with appropriate conditions on the two time parameters. Some key  $\gamma$ -ray coincidence spectra extracted from the list mode data are displayed in Fig. 1. The  $\gamma\gamma$  coincidence results demonstrated that the 86 keV transition occurs between the 0.5  $\mu\text{s}$  isomer at 2,919 keV and a shorter lived isomer at 2,833 keV, which de-excites to ground mainly through the 94, 390, 661, 1,688 keV  $\gamma$ -ray cascade. They also established a weaker 101, 383 keV branch in parallel with the 94, 390 keV section of the main cascade. The bottom-most spectrum in Fig. 1 identified the 1,061, 496 and 1,046 keV  $\gamma$ -rays as transitions occurring above the 0.5  $\mu\text{s}$  isomer; it was also found that the 496 keV transition is in prompt coincidence with both the 1,046 and 1,061 keV transitions.

The remaining measurements were performed using the more favorable  $^{136}\text{Ce}$  ( $^{16}\text{O}, 4n$ ) reaction, which gave greater  $^{148}\text{Dy}$  yields and much cleaner  $^{148}\text{Dy}$   $\gamma$ -ray spectra than the  $^{152}\text{Gd}(\alpha, 8n)$  reaction. In these experiments targets of  $>99\%$  enriched  $^{136}\text{Ce}$  (in oxide form, made in a Sidonic mass separator) were bombarded with beams of 85–95 MeV  $^{16}\text{O}$  ions from the Emperor Tandem at the MPI Heidelberg; recoiling nuclei were caught in Au or Al foils placed directly behind the targets. Most of the measurements utilized a 92 MeV beam pulsed in a 1  $\mu\text{s}$  on, 5  $\mu\text{s}$  off mode. A delayed  $\gamma$ -ray spectrum recorded in the intervals between beam bursts is shown in Fig. 2 with isotopic assignments indicated for all the strong  $\gamma$ -rays. Table 1 lists the energies of all the  $\gamma$ -rays assigned to  $^{148}\text{Dy}$ , together with their observed intensities in both  $(\alpha, 8n)$  and  $(^{16}\text{O}, 4n)$  reactions. Time distributions for several  $^{148}\text{Dy}$   $\gamma$ -rays obtained in a two-parameter measurement between the  $^{16}\text{O}$  beam bursts are shown in Fig. 3 (a); they give the half life for the 2,919 keV isomer

$$T_{1/2}(2,919 \text{ keV}) = 480 \pm 30 \text{ ns.}$$

Additional  $\gamma\gamma$  coincidence measurements were performed between the  $^{16}\text{O}$  beam bursts using 70 cm<sup>3</sup> Ge(Li) and 3''  $\times$  3'' NaI(Tl) detectors in 180° geometry. The  $t_{\gamma\gamma}$  data shown in Fig. 3b gave the half life for the 2,833 keV isomer in  $^{148}\text{Dy}$

$$T_{1/2}(2,833 \text{ keV}) = 65 \pm 20 \text{ ns.}$$

Examples of NaI spectra recorded in prompt coincidence with individual  $\gamma$ -ray Ge(Li) gates are shown in Fig. 4. These results, together with the measured  $\gamma$ -ray intensities, settled the placement of all transitions

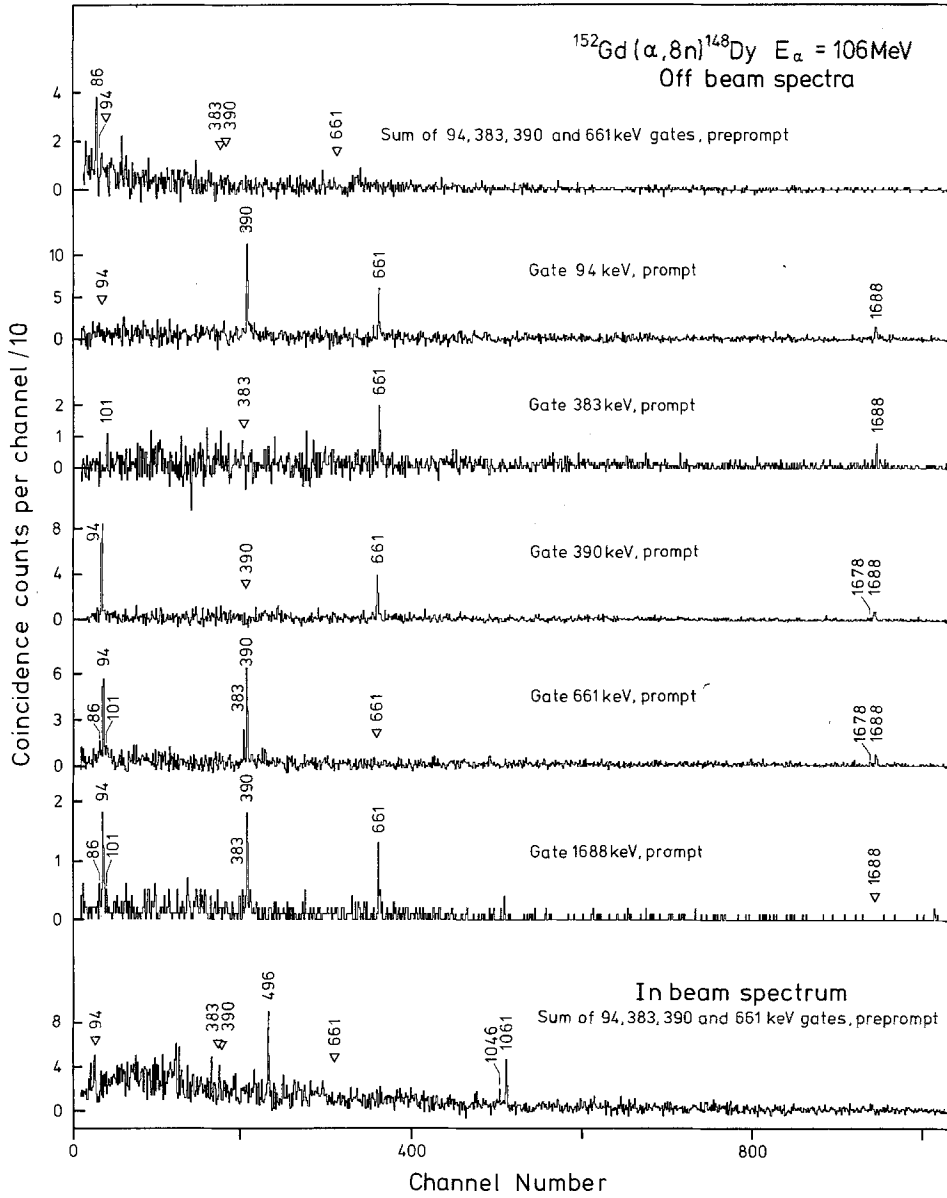


Fig. 1. Some important  $(\alpha, n)\gamma\gamma$  coincidence spectra. The five central spectra show prompt ( $\pm 10$  ns) coincidences with  $\gamma$  rays emitted during 80 ns intervals centered between the 120 ns separated beam bursts. In the other two spectra, labelled preprompt, the  $t_{12}$  condition was set to accept  $\gamma$ -rays preceding the gating transitions by 40 to 200 ns. In one case  $\gamma$ -rays emitted between beam bursts are shown, and in the other case those emitted during beam bursts

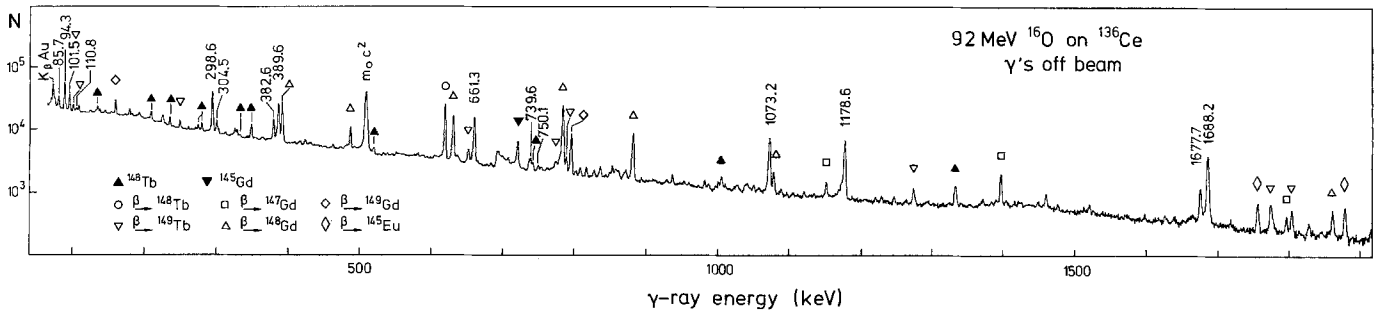


Fig. 2.  $\gamma$ -ray singles spectrum measured from 100 to 1,600 ns after  $1\ \mu\text{s}$  wide  $^{16}\text{O}$  beam bursts. Energies are given for  $^{148}\text{Dy}$  and  $^{149}\text{Dy}$  transitions

**Table 1.** Properties of Transitions in  $^{148}\text{Dy}$ 

$E_\gamma$ (keV)	Rel. $\gamma$ intensity <sup>a</sup>		$\alpha_K \times 10^2$	$\alpha_{\Sigma L}$	$\alpha_{\text{tot}}^c$	Multi- polarity	Placement	
	( $^{16}\text{O}, 4n$ ) 92 MeV	( $\alpha, 8n$ ) 106 MeV					$E_i$	$I_i \rightarrow I_f$
Transitions below the $10^+$ isomer								
85.7(4)	18	obsc.		2.9(4)	4.8(4)	E2	2,919.2	$10^+ \rightarrow 8^+$
94.3(4)	50	35(8)		<0.05	0.40(6)	E1	2,833.5	$8^+ \rightarrow 7^-$
101.5(3) <sup>b</sup>	$\sim 14^b$	12(4)		1.3(3)	1.9(4)	E2	2,833.5	$8^+ \rightarrow 6^+$
304.5(2)	13	13(3)	5(1)			E2	2,732.1	$6^+ \rightarrow 4^+$
382.6(2)	27	19(7)	1.1(3)			E1	2,732.1	$6^+ \rightarrow 5^-$
389.6(2)	70	66(9)	2.0(3)			E2	2,739.1	$7^- \rightarrow 5^-$
661.3(2)	88	88	0.60(7)			E2	2,349.5	$5^- \rightarrow 3^-$
739.6(3)	8.6		0.18(8)			E1	2,427.7	$4^+ \rightarrow 3^-$
750.1(4)	3.7		0.55(15)			E2	2,427.7	$4^+ \rightarrow 2^+$
1,677.7(7)	19	17	0.11(2)			E2	1,677.7	$2^+ \rightarrow 0^+$
1,688.2(7)	81	83	0.18(2)			E3	1,688.2	$3^- \rightarrow 0^+$
Transitions above the $10^+$ isomer								
				$A_2^c$	$A_4^c$			
495.9(2)	63	48(9) <sup>d</sup>	2.0(5)	-0.24(6)	-0.00(10)	M1(+E2)	4,476.2	$12^- \rightarrow 11^-$
1,045.6(2)	42	31(7)	0.23(3)	+0.22(10)	-0.16(14)	E2		
1,061.1(2)	65	53	0.08(1)	-0.15(5)	+0.00(7)	E1	3,980.3	$11^- \rightarrow 10^+$

<sup>a</sup> Unless otherwise specified intensity error  $\approx 10\%$ . For ( $^{16}\text{O}, 4n$ ) off beam intensities are given for transitions below the  $10^+$  isomer; inbeam intensities are listed for the above lying transitions and for ( $\alpha, 8n$ ).

<sup>b</sup> Data less certain due to poorly resolved 100.8 keV M1 transition from  $^{149}\text{Dy}$   $\beta$ -decay

<sup>c</sup> Measured in ( $\alpha, 8n$ ). Transitions below the  $10^+$  isomer were isotropic.

<sup>d</sup> Corrected for 31% contribution from degenerate line in  $^{150}\text{Gd}$

<sup>e</sup> From intensity balance

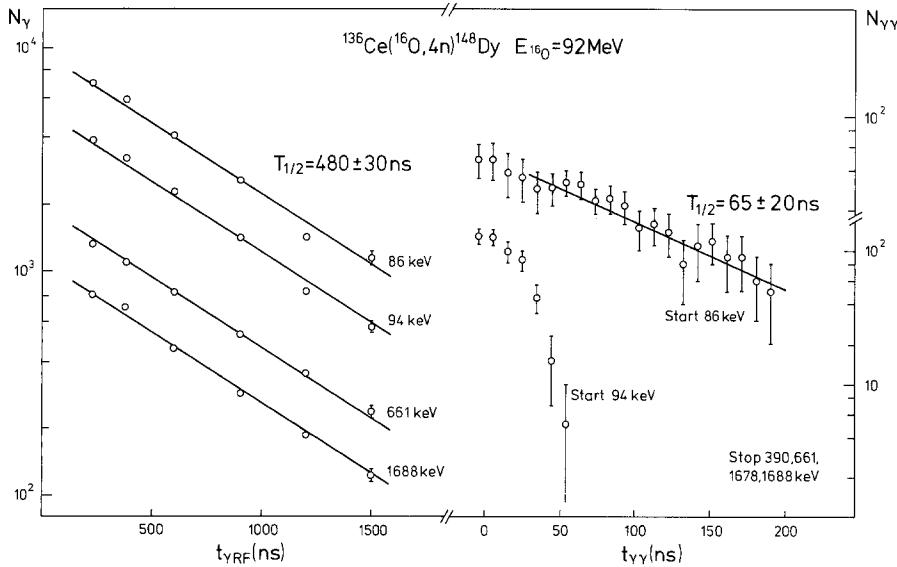


**Fig. 3.** Isomeric half lives in  $^{148}\text{Dy}$  measured with the pulsed  $^{16}\text{O}$  beam. **a** On the left is shown the half life of the 2.92 MeV  $10^+$  isomer obtained from  $\gamma$ -ray singles intensities between beam bursts. **b** On the right is shown the half life of the 2.83 MeV  $8^+$  isomer from a  $\gamma\gamma$  coincidence measurement, using a Ge(Li) as the start- and a NaJ as the stop detector. Only coincidences events during beam pauses were accepted

in  $^{148}\text{Dy}$  below the 480 ns isomer, and the resulting level scheme is shown in Fig. 8. It is noted that the coincidence results clearly showed the existence of an unobserved 10.5 keV transition between the 1,688 and 1,678 keV levels.

Conversion electron measurements were essential in order to determine transition multiplicities and thus the spins and parities of the established  $^{148}\text{Dy}$  levels.

These experiments were performed using specially prepared thin  $^{136}\text{Ce}$  targets and a solenoid spectrometer [13] operating in magnetic lens mode. The targets consisted of  $\sim 200 \mu\text{g}/\text{cm}^2$  of the  $>99\%$  enriched  $^{136}\text{Ce}$  deposited on  $\sim 30 \mu\text{g}/\text{cm}^2$  carbon foils by sputtering during collection in the mass separator. In the measurement, a  $^{136}\text{Ce}$  target was placed at  $45^\circ$  to the  $^{16}\text{O}$  beam direction and was backed by an Al foil,

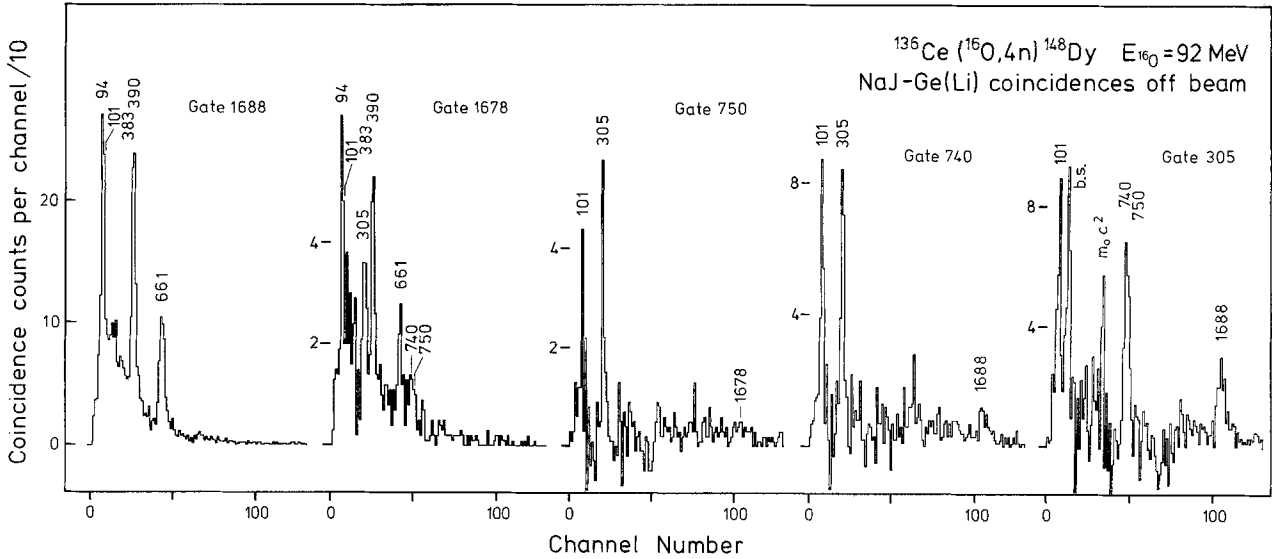


**Fig. 4.**  $\gamma\gamma$  coincidences measured between beam bursts with a  $70\text{ cm}^3$  Ge(Li) and a  $3'' \times 3''$  NaJ detector in  $180^\circ$  geometry. Gates are set on the Ge(Li) peaks, and coincident NaJ spectra are displayed. The 304 keV gate lies on the steep Compton edge of the 511 keV  $\beta^+$  decay radiation

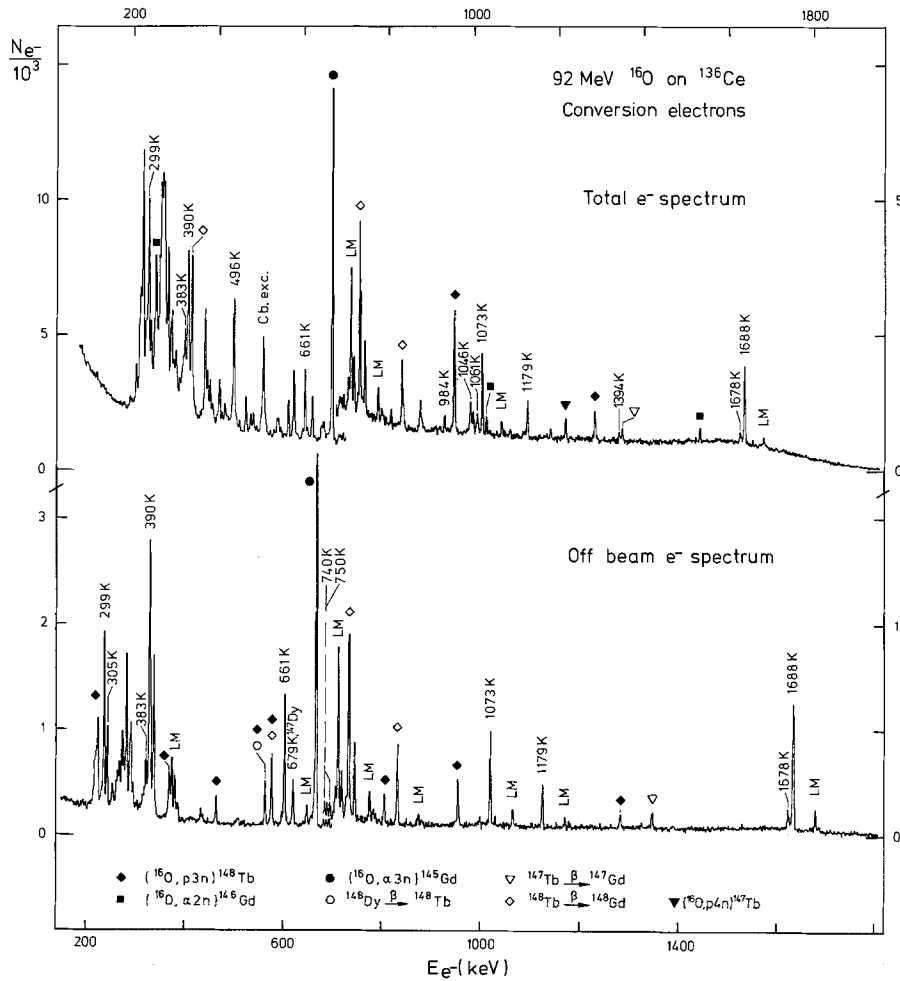


**Fig. 5.** Total- and off beam (100 to 1,600 ns after  $1\ \mu\text{s}$  beam bursts) electron spectra measured with the solenoid spectrometer [13] operated in lens mode. The solenoid current sweep covered the 280 to 1,680 keV electron energy range. Transition energies are given for the  $^{148}\text{Dy}$  and  $^{149}\text{Dy}$  lines. The K-line of the 679 keV  $M4$  transition in  $^{147}\text{Dy}$  is also labelled

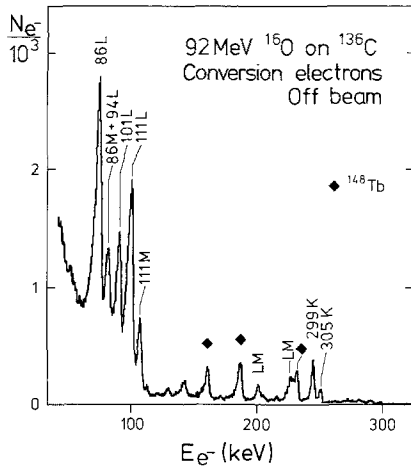


**Fig. 6.** Conversion electron spectrum for the 70 to 280 keV electron energy range measured in a similar manner as the lower one in Fig. 5

barely thick enough to stop the recoiling nuclei. Electrons were accepted in the  $10^\circ$  to  $20^\circ$  conical aperture of the lens spectrometer and were energy analysed in a cooled Si(Li) detector at the end of the solenoid. Both in-beam and out-of-beam electron spectra were recorded and representative samples of the data obtained are shown in Figs. 5 and 6. Conversion coefficients extracted from the electron and  $\gamma$ -

ray intensities are given in Table 1, and they are compared with theoretical conversion coefficients for various multiplicities in Fig. 7. For the three low energy transitions in  $^{148}\text{Dy}$ , total conversion coefficients were also deduced from the intensity balance requirements between the off-beam transition intensities. These results settled the multiplicities of all the  $^{148}\text{Dy}$  transitions below the 480 ns isomer including  $E1$  character for the 10.5 keV transition and established the spin-parity values shown in Fig. 8 for the  $^{148}\text{Dy}$  levels up to the  $10^+$  isomeric state.

It is clear that the 496 keV  $M1$  and 1,061 keV  $E1$  transitions occur in cascade into the  $10^+$  state, but the approximately equal intensities of these two transitions observed in both the  $(\alpha, 8n)$  and  $(^{16}\text{O}, 4n)$  reactions leaves a question about the transition ordering. The ordering shown in Fig. 8 is slightly, but not decisively, favored by the data; however as is discussed later, theoretical consideration of how the yrast line of  $^{148}\text{Dy}$  might continue above the  $10^+$  state strongly favors this transition ordering over the alternative.

## 2.2. The $^{149}\text{Dy}$ Level Scheme

Levels in the  $N = 83$  nucleus  $^{149}\text{Dy}$  were also strongly populated in the  $^{16}\text{O}$  ion bombardments of  $^{136}\text{Ce}$

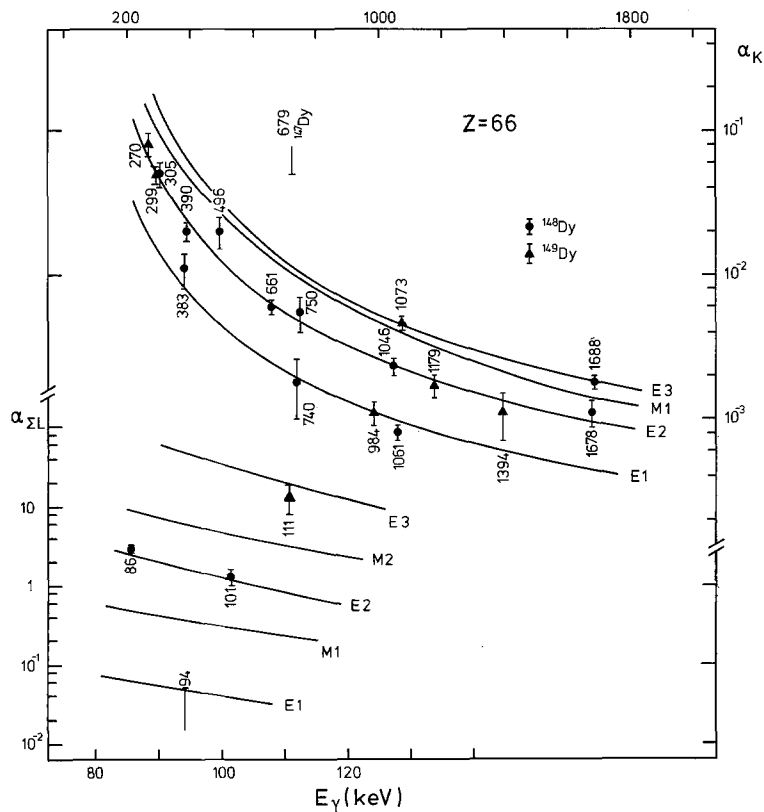


**Fig. 7.** A comparison of the measured conversion coefficients for transitions in  $^{148}\text{Dy}$  and  $^{149}\text{Dy}$  with theoretical values. For the 679 keV transition of  $^{147}\text{Dy}$  the data gave  $\alpha_K > 5 \times 10^{-2}$  consistent with  $M3$ ,  $M4$ , or higher multiplicities

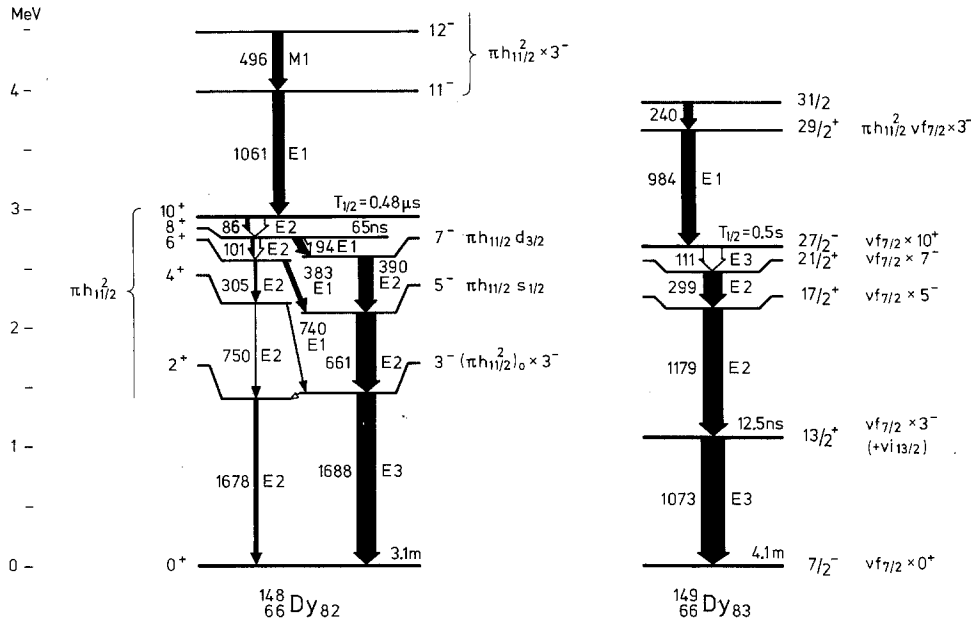


**Fig. 8.** Level schemes for  $^{148}\text{Dy}$  and  $^{149}\text{Dy}$  with proposed shell model configuration assignments. Transition intensities are those measured in-beam in the  $(\alpha, 8n)$  and  $(\alpha, 7n)$  reactions. All multiplicities shown have been determined from conversion coefficient measurements. Level energies and more precise transition energies are listed in Tables 1 and 2

and it was possible to extract from the data valuable new information about transitions in  $^{149}\text{Dy}$ . In addition, new lifetime measurements for  $^{149}\text{Dy}$  were performed using the  $^{152}\text{Gd}(\alpha, 7n)$  reaction, and more detailed sorting of our old  $^{149}\text{Dy}$   $\gamma\gamma$  coincidence data was also fruitful. The results of these experiments established that all the transitions listed as “probable”  $^{149}\text{Dy}$   $\gamma$ -rays in [6] certainly occur above the  $27/2^-$  isomer in this nucleus and a few other high-lying  $^{149}\text{Dy}$  transitions were also identified.

Table 2 summarizes the properties of the transitions assigned to  $^{149}\text{Dy}$ , including conversion coefficients determined from the electron and  $\gamma$ -ray intensities in the  $^{136}\text{Ce}(^{16}\text{O}, 3n)$  reaction. These conversion coef-

ficients are also compared with theory in Fig. 7 and the inferred transition multiplicities are given in Table 2. For the four transitions below the 0.5 s isomer the present results confirm the multiplicities deduced earlier from less conclusive evidence. Consequently, the  $I^\pi$  values shown in Fig. 8 for the  $^{149}\text{Dy}$  levels up to the  $27/2^-$  isomer can now be considered certain. The half life of the  $13/2^+$  state at 1,073 keV has been determined to be

$$T_{1/2}(1,073 \text{ keV}) = 12.5 \pm 1.5 \text{ ns}$$

corresponding to a  $B(E3)$  value of  $45 \pm 5$  Weisskopf units.

**Table 2.** Properties of Transitions in  $^{149}\text{Dy}$

$E_\gamma$ (keV)	Rel. $\gamma$ intensity <sup>a</sup>		$\alpha_K \cdot 10^2$	$A_2$	$A_4$	Multi- polarity	Placement	
	$(^{16}\text{O}, 3n)$ 92 MeV	$(\alpha, 7n)$ 106 MeV					$E_i$	$I_i \rightarrow I_f$
Transitions below the $27/2^-$ isomer								
110.8(4)		$\sim 3^b$	13(5) <sup>c</sup>			E3	2,661.2	$27/2^- \rightarrow 21/2^+$
298.6(1)	80	83	4.9(7)			E2	2,550.4	$21/2^+ \rightarrow 17/2^+$
1,073.2(2)	100	100	0.46(5)			E3	1,073.2	$13/2^+ \rightarrow 7/2^-$
1,178.6(1)	95	91	0.17(3)			E2	2,251.8	$17/2^+ \rightarrow 13/2^+$
Transitions above the $27/2^-$ isomer								
199.4(3)	50(10)	20(6)		-0.19(4)	-0.05(5)			
240.0(3)	80(20)	39(6)		-0.20(5)	0.00(6)		3,885.5	$31/2 \rightarrow 29/2^+$
255.0(2)	32(9)	$\sim 6^b$						
270.0(2)	42	15(3)	8.0(1.5)	-0.04(5)	-0.01(8)	(M1+E2)		
430.3(2)	43(8)	18(6)						
984.3(2)	78	61	0.11(2)	-0.18(3)	+0.00(4)	E1	3,645.5	$29/2^+ \rightarrow 27/2^-$
1,337.2(4)	35(6)	18(3)		+0.19(9)	-0.02(9)			
1,393.7(5)	30	18(4)	0.11(4)			E2		

<sup>a</sup> Unless specified otherwise intensity error  $\approx 10\%$ . In-beam intensities listed for both reactions.

<sup>b</sup> Estimated from coincidence data.

<sup>c</sup> Value listed is  $\alpha_{SL}$ , extracted from Fig. 6 via comparison with 299 K line intensity.

The present results also establish that the cascade of 240 and 984 keV transitions populates the  $27/2^-$  isomer, and the  $(\alpha, 7n)$  singles  $\gamma$ -ray intensities show that the 984 keV transition is lower lying. Since the conversion coefficient and angular distribution results clearly indicate stretched  $E1$  character for the 984 keV transition, the next yrast state above the  $27/2^-$  isomer is a  $29/2^+$  level at 3,645 keV. The 240 keV dipole transition de-excites a level at 3,885 keV, and the other transitions in Table 2 occur above this level.

Finally, the half life of the higher-lying isomer first reported in [6] has been redetermined to be  $36 \pm 8$  ns. This isomer has also been observed recently by other workers [14–16], but the excitation energy and spin-parity of the isomeric state are still unknown.

### 3. Discussion

#### 3.1. The Nucleus $^{148}\text{Dy}$

In [9] we have already commented on the energy systematics of the lowest  $2^+$  and  $3^-$  states in the  $N=82$  isotones and have pointed out that the location of the  $^{148}\text{Dy}$   $2^+$  state at a much lower energy than the  $^{146}\text{Gd}$  1,972 keV  $2^+$  state lends support to earlier arguments for the  $Z=64$  shell closure. Since the dominant component of the  $3^-$  octupole excitation at  $N=82$  is  $\pi h_{11/2} d_{5/2}^{-1}$ , involving the promotion of a proton across the  $Z=64$  gap, the  $3^-$  energy is as expected lowest in  $^{146}\text{Gd}$ , and somewhat higher in  $^{148}\text{Dy}$ , where the Fermi surface is displaced upwards. Later in this section the  $3^-$  energies will be examined from another viewpoint.

The rate of the 10 keV  $3^- \rightarrow 2^+$   $E1$  transition is  $2 \times 10^{-3}$  Weisskopf units, assuming that the  $3^- \rightarrow 0^+$   $E3$  transition rate is 37 Weisskopf units as in  $^{146}\text{Gd}$  [17]. We note that the corresponding  $E1$  transition [18] in the  $N=82$  two proton hole nucleus  $^{144}\text{Sm}$  is

equally fast. Rates of  $3^- \rightarrow 2^+$   $E1$  transitions in other spherical nuclei in the Zr and Pb regions are of similar magnitude.

*3.1.1. The  $\pi h_{11/2}^2$  Spectrum and the  $\pi h_{11/2}$  Effective Charge.* The  $10^+$  isomer at 2,919 keV in  $^{148}\text{Dy}$  is without doubt the fully aligned  $\pi h_{11/2}^2$  state, and all other members of the  $\pi h_{11/2}^2$  multiplet are also identified in this study. The levels with  $I \geq 6$ , and especially the  $8^+$  and  $10^+$  states, should have exceptionally pure  $\pi h_{11/2}^2$  configurations, since the only other available single proton states are  $s_{1/2}$  and  $d_{3/2}$  above the gap, and  $d_{5/2}$  and  $g_{7/2}$  below the gap. Examples of such complete  $j^2$  spectra are rather rare, and thus far include no other case with  $j > 9/2$ .

The energy spectra of nuclei with two valence nucleons are prime sources of information about two nucleon residual interactions, essential for many shell model applications. There have been several attempts to fit the interaction matrix elements derived from the experimental data. Of particular note is the extensive analysis by Schiffer and True [19] of all the known  $T=0$  and  $T=1$  matrix elements, which elucidated the universal properties of the nucleon-nucleon residual interaction throughout the nuclear chart. The present study provides the first information about residual interactions for two  $h_{11/2}$  protons. It is instructive to compare these results with the other known cases of two identical valence particles in the same  $j$ -shell, with nodeless radial wave functions (Fig. 9).

The  $0^+$  ground states in all six nuclei have admixtures from other configurations. In particular, a large  $\pi p_{1/2}^2$  contribution to the  $^{90}\text{Zr}$  ground state has been established [20] from single nucleon transfer data, and one expects a similar situation in  $^{148}\text{Dy}$  with the  $\pi s_{1/2}^2$  and  $\pi d_{3/2}^2$  configurations contributing substantially to the ground state. The clustering of the  $h_{11/2}$ ,  $s_{1/2}$  and  $d_{3/2}$  states in the single particle diagram above  $Z=64$  contrasts with the situation above the  $Z$

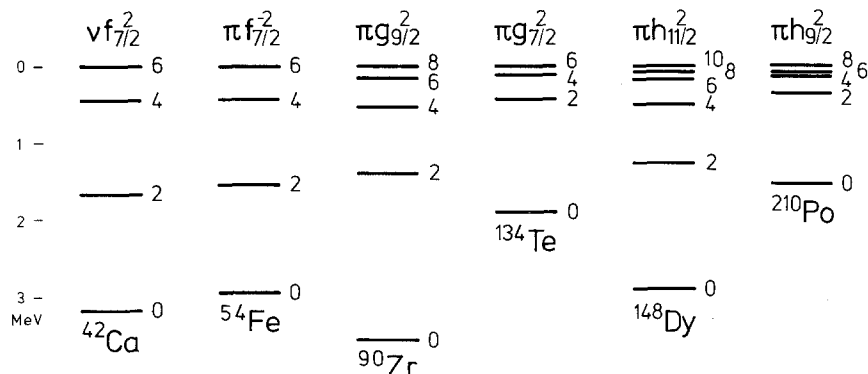


Fig. 9. A comparison of  $j^2$ -spectra for nuclei with two identical valence nucleons



= 50 and  $Z=82$  gaps where the lowest single particle states are well separated from other orbitals.

The lowering of the  $0^+$  levels in these  $j^2$  spectra is largely determined by the pairing interaction. The energy of the  $0^+$  ground state relative to the top of the  $j^2$  spectrum can be written as

$$\delta E(0) = G_{\text{eff}} \Omega,$$

where  $G_{\text{eff}}$  is an effective pair coupling constant,  $G_{\text{eff}} = cA^{-1}$ , and  $\Omega$  is the pair degeneracy of the single  $j$  shell,  $\Omega = j + \frac{1}{2}$ . For the four heaviest nuclei the strength parameter  $c$  is about 65 MeV, which is 2 to 3 times larger than standard values [21] used in BCS calculations within an entire major shell. This shows that several orbitals must contribute substantially to the  $0^+$  lowering. The variation of  $\delta E(0)$  with  $A$  and  $j$  is, however, well reproduced by the  $A^{-1}(j + \frac{1}{2})$  dependence, indicating that in these four cases the enhancement due to other orbitals than the leading one is constant within 10 %.

As is well known, the energy levels of  $j^2$  spectra, such as those in Fig. 9, can be roughly reproduced by considering only a short range force between the two nucleons. A delta force, for example, is often used in first approximation. However, the observed multiplet members are invariably more widely spread apart than is calculated using a  $\delta$ -force; particularly, the  $2^+$  level is always found at a lower energy than the  $\delta E(2)/\delta E(0) \simeq 1/4$  given by this force. One simple method that has been used to improve the agreement with experiment is to add to the  $\delta$ -force a long range quadrupole component mediated by the core. It is apparent from the relative energies of the  $2^+$  states in Fig. 9 that the quadrupole component must be considerably stronger in  $^{148}\text{Dy}$  than in  $^{134}\text{Te}$  and  $^{210}\text{Po}$ . This may be attributed to the fact that the  $Z=64$  gap lies within the  $N=4$  oscillator shell, giving rise to the low-lying  $\Delta N=0$   $2^+$  excitation [22] at 2 MeV in the  $^{146}\text{Gd}$  core, whereas the corresponding  $2^+$  states in the  $^{132}\text{Sn}$  [23] and  $^{208}\text{Pb}$  core nuclei lie above 4 MeV. The  $^{148}\text{Dy}$  spectrum more closely resembles that of  $^{90}\text{Zr}$ , where the  $2^+$  state of the  $^{88}\text{Sr}$  core nucleus also occurs at about 2 MeV.

In any case, the empirical  $h_{11/2}^2$  two particle energies now determined from the spectrum of  $^{148}\text{Dy}$  provide essential input information for calculation of more complex multiparticle configurations in the  $A \sim 150$  region. Furthermore the excitation energy of the  $10^+$  state is vital information for the determination [10] of the  $^{148}\text{Dy}$  mass.

The effective charge of the  $h_{11/2}$  proton can be calculated from the measured rate of the  $10^+ \rightarrow 8^+$  transition in  $^{148}\text{Dy}$ . Using the radial matrix element

$$\langle r^2 \rangle_N = 0.93 A^{1/3} (N + 3/2) = 32 \text{ fm}^2$$

and the assumption that only two protons occupy the  $h_{11/2}$  shell, we obtain

$$B(E2, 10^+ \rightarrow 8^+) = 43 \pm 3 e^2 \text{ fm}^4$$

and

$$e_{\text{eff}} = 1.52 \pm 0.05 e.$$

The rate for the  $8^+ \rightarrow 6^+$  transition is subject to large experimental uncertainties in both the half life and the branching ratio but gives an effective charge consistent with the above value.

This result is similar to the effective charges found for the two-proton nuclei

$$\begin{aligned} ^{134}\text{Te} \quad \pi g_{7/2}^2(6 \rightarrow 4); \quad e_{\text{eff}} = 1.5 \pm 0.1 e \quad [24] \quad \text{and} \\ ^{210}\text{Po} \quad \pi h_{9/2}^2(8 \rightarrow 6); \quad e_{\text{eff}} = 1.5 \pm 0.1 e \quad [8, 25]. \end{aligned}$$

As we have just discussed in connection with the  $j^2$  energy spectra, the quadrupole polarizability appears to be distinctly larger in  $^{146}\text{Gd}$  than in the  $^{132}\text{Sn}$  and  $^{208}\text{Pb}$  cores. Such increased quadrupole softness should also result in enhanced effective  $E2$  charges, and the similar results obtained in the three cases are at first sight unexpected. However, the  $^{146}\text{Gd}$   $2^+$  excitation differs markedly from those of  $^{132}\text{Sn}$  and  $^{208}\text{Pb}$  in that its structure is dominated by proton components [1]. Because of the strong isospin dependence of core polarization, valence protons should be less effective in polarizing the  $^{146}\text{Gd}$  core than valence neutrons, and accordingly the coupling to the  $^{146}\text{Gd}$   $2^+$  state should be most clearly manifested in the enhancement of neutron effective charges. First results [26, 27] in  $N=84$  and  $N=85$  nuclei indeed indicate substantially enhanced effective charges for the valence neutrons, but a more detailed study of this whole question is desirable.

**3.1.2. Negative Parity States.** The lowest  $5^-$  and  $7^-$  states in  $^{146}\text{Gd}$  are mainly of  $\pi h_{11/2} d_{5/2}^{-1}$  character [1], and corresponding  $ph$  excitations are expected in  $^{148}\text{Dy}$  at somewhat higher excitation energies. However, the  $5^-$  and  $7^-$  states observed in  $^{148}\text{Dy}$  lie  $\sim 0.3$  MeV lower than the  $^{146}\text{Gd}$   $5^-$ ,  $7^-$  states; we conclude that they must have different structures. Two particle excitations of the type  $\pi h_{11/2} s_{1/2}$  and  $\pi h_{11/2} d_{3/2}$  should occur at low energies in Dy, and we interpret the 2,350 and 2,739 keV levels in  $^{148}\text{Dy}$  as predominantly  $(\pi h_{11/2} s_{1/2}) 5^-$  and  $(\pi h_{11/2} d_{3/2}) 7^-$  states, the expected lowest-lying (singlet coupling) members of the two multiplets.

**3.1.3. Octupole Excitations.** At  $I=10$  the  $^{148}\text{Dy}$  valence spin is exhausted and higher yrast states must involve breaking of the  $^{146}\text{Gd}$  core. Since the  $3^-$  octupole is the lowest core excitation, the yrast line

can be expected to continue by excitations of the type  $10^+ \times 3^-$ . In the experiment, the strong 1,061 keV  $E1$  transition is found to populate the  $^{148}\text{Dy}$   $10^+$  isomer from a 3,980 keV  $11^-$  level, which we interpret as the lowest member of the octupole multiplet built on the  $\pi h_{11/2}^2 10^+$  state.

Our recent analysis [2] of the related but simpler situation in the  $Z=65$  nucleus  $^{147}\text{Tb}$  has provided valuable insight, preparing the way for understanding the  $h_{11/2}^2 \times 3^-$  coupling in  $^{148}\text{Dy}$ . The  $^{147}\text{Tb}$  nucleus has one  $h_{11/2}$  proton in its ground state and the lowest octupole state with  $I^\pi=15/2^+$  is connected to the ground state by  $\Delta I=2$  transitions. This finding can be understood as a consequence of the Pauli interference with the large  $\pi h_{11/2} d_{5/2}^{-1}$  component of the core octupole, and the data have been successfully analyzed in terms of particle core exchange interaction. In the  $^{148}\text{Dy}$   $10^+$  state at 2,919 keV, two  $h_{11/2}$  protons are aligned and in this case one can expect the lowest member of the octupole multiplet to be two units in spin less than the maximally aligned  $13^-$  member. The particle-phonon exchange diagram appropriate to the  $^{148}\text{Dy}$   $\pi h_{11/2}^2 \times 3^-$  coupling, with three  $h_{11/2}$  particles and one  $d_{5/2}$  hole in the intermediate state, is shown in Fig. 10; the  $^{147}\text{Tb}$

case is also illustrated for purposes of comparison. In second order perturbation theory, the energy shifts for members of the octupole multiplet in  $^{148}\text{Dy}$  are given by

$$\begin{aligned} \delta E((h_{11/2}^2)_I \times 3^-; I) \\ = 14(2I+1) \times X \left( \frac{11}{2} \frac{11}{2} I'; \frac{11}{2} \frac{5}{2} 3; I' 3I \right) \\ \times \frac{\langle (h_{11/2} d_{5/2})_3 | H | 3^- \rangle^2}{E(h_{11/2}) - E(d_{5/2}) - E_{3^-}} \end{aligned}$$

where  $X$  is a  $9j$  symbol, and  $I'$  specifies the coupling of the two  $h_{11/2}$  protons in the initial state. The crucial point here is that the energy factor  $\langle |H| \rangle^2 / \Delta E$  containing the interaction matrix element is the same as in the  $^{147}\text{Tb}$  case, and therefore one can use the empirical energy factor from the one-particle phonon coupling to describe the exchange interaction of two particles with the phonon. With the value of 856 keV for that energy factor, derived from the observed 772 keV splitting of the  $15/2^+$  and  $17/2^+$  levels in  $^{147}\text{Tb}$ , we have calculated the expected energy shifts for the four highest spin members of the  $h_{11/2}^2 \times 3^-$  multiplet in  $^{148}\text{Dy}$ . (The  $I'=10$  and 8 couplings both contribute to the  $11^-$  and  $10^-$  states, and the theoretical energies shown are the lower energy solutions obtained by diagonalizing the interaction in this two-dimensional basis.) In Fig. 10 the calculated level energies are compared with the experimental results. The good agreement with the observed  $11^-$ ,  $12^-$  energies provides strong support for the interpretation of these states as octupole multiplet members. In future experiments it may be possible to locate additional members of the  $h_{11/2}^2 \times 3^-$  multiplet, particularly the  $13^-$  member which should be an yrast state.

The fact that the excitation energy of the  $3^-$  octupole state is higher in  $^{148}\text{Dy}$  than in  $^{146}\text{Gd}$  can also be understood as a Pauli interference effect. In this case, the geometrical blocking coefficient  $14(2I+1)X$  for  $I'=0$  equals  $2/12$  assuming that two of the twelve  $h_{11/2}$  protons are present in the  $^{148}\text{Dy}$   $0^+$  ground state. With the same empirical matrix element, the calculated energy shift is  $\delta E = +143$  keV, which is close to the experimental number of

$$E_{3^-}(^{148}\text{Dy}) - E_{3^-}(^{146}\text{Gd}) = 109 \text{ keV.}$$

As mentioned earlier, the proton pair in the  $^{148}\text{Dy}$  ground state also partially occupies the  $s_{1/2}$  and  $d_{3/2}$  orbitals, and therefore this slightly smaller increase of the  $3^-$  energy in  $^{148}\text{Dy}$  is not unexpected.

As far as we know, this type of particle phonon exchange coupling involving two particles has not been observed before; it is encouraging that the em-

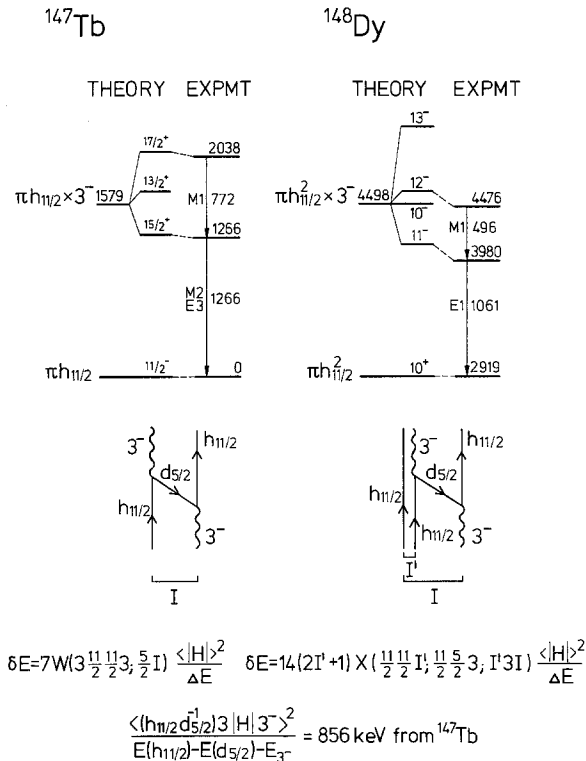


**Fig. 10.** One-particle phonon and two-particle phonon exchange coupling involving the 1,579 keV octupole excitation in the  $^{146}\text{Gd}$  core. Experimental and calculated  $\pi h_{11/2} \times 3^-$  and  $\pi h_{11/2}^2 \times 3^-$  multiplet members in  $^{147}\text{Tb}$  and  $^{148}\text{Dy}$  are shown

pirical coupling strength derived from the one-particle case describes the more complex situation so well.

### 3.2. The Nucleus $^{149}\text{Dy}$

Earlier [6, 7], we established the  $^{149}\text{Dy}$  level scheme up to the  $27/2^-$  isomer at 2,661 keV. In the following sections we discuss some important aspects of the  $^{149}\text{Dy}$  level structure in the light of recent results for neighbouring nuclei, especially  $^{148}\text{Dy}$ , and we also consider the extension of the  $^{149}\text{Dy}$  yrast line beyond the  $27/2^-$  isomer.

**3.2.1. The  $13/2^+$  Octupole Excitation.** We originally [6] interpreted the 1,073 keV  $13/2^+$  level as an  $\nu i_{13/2}$  single particle excitation. In subsequent work, much has been learned about octupole excitations in this region, most notably the correct identification [28] of the  $^{146}\text{Gd}$   $3^-$  state and the determination [17] of its  $B(E3)$  value. For the  $^{149}\text{Dy}$   $13/2^+$  level the measured half-life gives

$$B(E3) = (5.9 \pm 0.7) \times 10^4 e^2 \text{ fm}^6 \quad \text{or} \quad 45 \pm 5 \text{ W.u.}$$

which is close to the value for the  $^{146}\text{Gd}$  octupole. Similar  $E3$  strengths have also been determined [1, 2] for low-lying octupole excitations in  $^{147}\text{Gd}$ ,  $^{147}\text{Tb}$  and  $^{148}\text{Tb}$ , and it is now clear that the 1,073 keV state in  $^{149}\text{Dy}$  is predominantly an octupole excitation built on the  $\nu f_{7/2}$  ground state.

A similar interpretation is also indicated for the lowest lying  $13/2^+$  levels [29] in other  $N=83$  nuclei. As shown in Fig. 11, the energies of the  $13/2^+$  states in the  $N=83$  isotones closely follow those of the  $3^-$  states in the corresponding  $N=82$  nuclei; this contrasts with the energy trend observed for the  $\nu h_{9/2}$  levels, which are probably much purer single particle excitations. While a large contribution of  $\nu i_{13/2}$  single

particle character is definitely indicated by the fact that the  $13/2^+$  states lie  $\sim 0.6$  MeV lower than the corresponding  $3^-$  core states, we conclude that the low-lying  $13/2^+$  excitations in  $N=83$  nuclei are predominantly  $\nu f_{7/2} \times 3^-$ .

The situation in the  $N=83$  isotones is basically similar to that observed in the  $N=127$  nucleus  $^{209}\text{Pb}$ , where the corresponding single particle orbits are  $\nu g_{9/2}$  and  $\nu j_{15/2}$ . In  $^{209}\text{Pb}$  a quantitative analysis [30] shows that the  $15/2^+$  state at 1.42 MeV is mostly of  $\nu j_{15/2}$  single particle character with about 30% admixture of  $\nu g_{9/2} \times 3^-$ . In  $^{147}\text{Gd}$  a similar analysis indicates that the unperturbed energy of  $\nu i_{13/2}$  is higher than that of  $\nu f_{7/2} \times 3^-$ . The situation is therefore reversed compared to  $^{209}\text{Pb}$ , and the physical  $13/2^+$  state is mostly of  $\nu f_{7/2} \times 3^-$  character with about 30% admixture of  $\nu i_{13/2}$ . The measured  $g$ -factor [31] of the  $13/2^+$  state in  $^{147}\text{Gd}$  is consistent with this mixed structure.

Of some interest for the yrast spectroscopy of nuclei in this region is the unperturbed  $\nu i_{13/2}$  single particle energy, which is not directly determined by experiments. The above analysis and other evidence from spectroscopic studies [2, 26, 32] of various Gd and Tb nuclei indicates that it lies more than 2 MeV above the  $\nu f_{7/2}$  ground state, and thus higher than the  $^{146}\text{Gd}$   $3^-$  octupole excitation. The energy systematics of Fig. 11 also points towards the same conclusion. In  $^{149}\text{Dy}$ , with two valence protons, residual  $np$  interactions should cause a significant lowering of the  $\nu i_{13/2}$  energy similar to that observed for the  $\nu h_{9/2}$  single particle state, which drops from 1,398 keV in  $^{147}\text{Gd}$  to 1,091 keV in  $^{149}\text{Dy}$ . However from the very regular  $13/2^+$  energy systematics, we infer that also in the  $^{149}\text{Dy}$  nucleus the  $\nu i_{13/2}$  single particle state should be located above the octupole. That the  $\nu i_{13/2}$  single particle energy at  $N=83$  is so high has not previously been clearly recognized. It would explain why  $i_{13/2}$  neutrons rarely play a role in the yrast lines of  $A \approx 150$  nuclei, whereas the  $\nu h_{9/2}$  single particle excitation frequently contributes to yrast configurations.

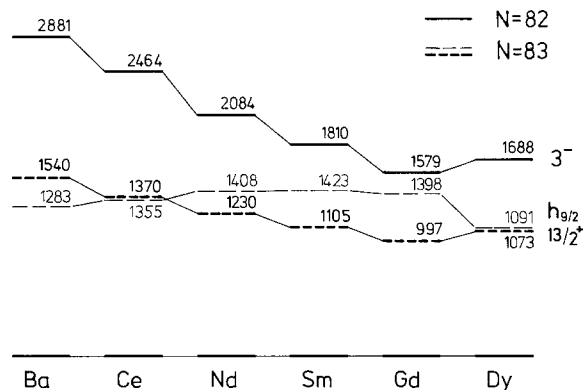


**Fig. 11.** Energy systematics of  $3^-$  levels in  $N=82$ , and ( $\nu f_{7/2} \times 3^-$ )  $13/2^+$  and  $\nu h_{9/2}$  levels in  $N=83$  isotones

**3.2.2. The  $17/2^+$ ,  $21/2^+$  and  $27/2^-$  States.** In our earlier study [6, 7] we interpreted the  $27/2^-$  isomeric state as  $(\pi h_{11/2}^2)_{10} \times \nu f_{7/2}$ , but at that time the nature of the  $17/2^+$  and  $21/2^+$  levels remained unclear. We now identify them as states arising from the coupling of the  $f_{7/2}$  neutron with the  $5^-$  and  $7^-$  states of  $^{148}\text{Dy}$ , with the three-particle configurations  $(\pi h_{11/2} s_{1/2} \nu f_{7/2}) 17/2^+$  and  $(\pi h_{11/2} d_{3/2} \nu f_{7/2}) 21/2^+$  as dominant amplitudes. However, the  $\pi h_{11/2} \rightarrow d_{3/2}$  single particle jump implied for the  $27/2^- \rightarrow 21/2^+$   $E3$  transition is forbidden. In this region the most likely allowed  $E3$  transition is  $\pi h_{11/2} \rightarrow d_{5/2}^-$ , and its trans-

ition rate is known [33] from  $^{145}\text{Eu}$  to be

$$B(E3, h_{11/2} \rightarrow d_{5/2}^{-1}, ^{145}\text{Eu}) = 0.4 \times 10^4 e^2 \text{ fm}^6.$$

From the much slower transition rate observed in  $^{149}\text{Dy}$

$$B(E3, 110.8 \text{ keV}, ^{149}\text{Dy}) = 0.04 \times 10^4 e^2 \text{ fm}^6$$

we conclude that the  $(\pi h_{11/2}^3 d_{5/2}^{-1} \nu f_{7/2})$  configuration contributes of the order of 10 % to the  $21/2^+$  state in  $^{149}\text{Dy}$ . The small  $B(E3)$  value of the 111 keV transition thus supports the  $(\pi h_{11/2} d_{3/2} \nu f_{7/2})$  assignment for the  $21/2^+$  state and indicates also that the  $(\pi h_{11/2}^3 d_{5/2}^{-1})$  configuration contributes little to the composition of the  $^{148}\text{Dy } 7^-$  state.

As will be shown in [10], the measured excitation energy of the  $27/2^-$  state provides useful information for estimating the ground state masses of nuclei in this region.

**3.2.3. High-lying Particle plus Octupole Excitation.** We interpret the 3,645 keV  $29/2^+$  level, which de-excites by the 984 keV  $E1$  transition to the  $27/2^-$  isomer, as the counterpart of the  $(\pi h_{11/2}^2 \times 3^-)$   $11^-$  level at 3,980 keV in  $^{148}\text{Dy}$ . Its configuration is thus  $(\pi h_{11/2}^2 \nu f_{7/2} \times 3^-)$   $29/2^+$ . Again, the spin of the lowest octupole multiplet member is two units less than the highest possible spin because of Pauli interference with the two aligned  $h_{11/2}$  protons. Whether other multiplet members are populated in the yrast decay is at present not clear; in analogy to the isotope  $^{148}\text{Tb}$ , one would expect that levels of  $\pi h_{11/2}^2 \nu i_{13/2}$  nature might also occur in this region of the  $^{149}\text{Dy}$  yrast line.

It is noteworthy that similar  $\Delta I=1$  transitions from octupole states also occur in the yrast lines of heavier Dy nuclei. For example, in  $^{150}\text{Dy}$  a 742 keV  $E1$  transition de-excites [34] the 5,813 keV  $19^-$  octupole state to the  $(\pi h_{11/2}^2 \nu f_{7/2} h_{9/2}) 18^+$  level, and in  $^{151}\text{Dy}$  the  $(\pi h_{11/2}^2 \nu h_{9/2} f_{7/2}^2) 41/2^-$  state is fed [14, 35] by an 839 keV  $E1$  from the  $(41/2^- \times 3^-) 43/2^+$  yrast state at 5,743 keV. In all cases these octupole excitations are built on yrast states in which all available  $\pi h_{11/2}$ ,  $\nu f_{7/2}$  and  $\nu h_{9/2}$  valence spins are fully aligned. The fact that octupole core excitation competes successfully with lifting of a neutron into the  $\nu i_{13/2}$  orbital reemphasizes the rather high single particle energy of that orbital discussed above.

#### 4. Conclusion

This investigation has established the yrast level spectra of the  $N=82$  and  $83$  nuclei  $^{148}\text{Dy}$  and  $^{149}\text{Dy}$  to about 4 MeV excitation energy. A complete  $\pi h_{11/2}^2$

spectrum in  $^{148}\text{Dy}$  has been identified, providing the relative residual interaction matrix elements for two  $h_{11/2}$  protons. The determination of the  $\pi h_{11/2} E2$  effective charge gives valuable information about the polarizability of the  $^{146}\text{Gd}$  core nucleus. Of particular interest is the first observation of particle phonon exchange coupling involving two particles, and its successful description using an empirical interaction strength extracted from the simpler coupling in the one valence particle nucleus  $^{147}\text{Tb}$ . The  $^{148}\text{Dy}$  and  $^{149}\text{Dy}$  yrast lines are particularly favourable for the observation of such particle-phonon exchange phenomena because the high- $j$   $h_{11/2}$  protons, which are here valence particles, are also involved in the dominant component of the  $^{146}\text{Gd}$  core octupole. Similar octupole excitations also occur in heavier Dy nuclei, and related coupling phenomena should also play an important role in the yrast spectra of nuclei above dysprosium.

We thank L. Richter, Y. Nagai, M. Ogawa, M. Piiparinen and A. Stefanini for their assistance in some of the measurements, and R. Wagner for preparing the enriched target materials, especially the thin  $^{136}\text{Ce}$  targets vital for the conversion electron measurements. Fruitful discussions with O. Schult are also gratefully acknowledged.

#### References

1. Kleinheinz, P., Broda, R., Daly, P.J., Lunardi, S., Ogawa, M., Blomqvist, J.: *Z. Phys. A* **290**, 279 (1979)
2. Broda, R., Behar, M., Kleinheinz, P., Daly, P.J., Blomqvist, J.: *Z. Phys. A* **293**, 135 (1979)
3. Haenni, D.R., Beuscher, H., Lieder, R.M., Müller-Veggian, M., Neskakis, A., Mayer-Böricke, C.: *Proceedings of the International Conference on Structure of Medium-Heavy Nuclei*, Rhodos, p. 133. (1979)
4. Haenni, D.R., Beuscher, H., Lieder, R.M., Müller-Veggian, M., Neskakis, A., Mayer-Böricke, C.: *Nucl. Phys. A* **331**, 141 (1979)
5. Bazzacco, D., Hague, A.M.I., Zell, K.O., von Brentano, P., Protop, C.: *Phys. Rev. C* **21**, 222 (1980)
6. Stefanini, A.M., Daly, P.J., Kleinheinz, P., Maier, M.R., Wagner, R.: *Nucl. Phys. A* **258**, 34 (1976)
7. Stefanini, A.M., Kleinheinz, P., Maier, M.R.: *Phys. Lett.* **62B**, 405 (1976)
8. Häusser, O., Alexander, T.K., Beene, J.R., Earle, E.D., McDonald, A.B., Khanna, F.C., Towner, I.S.: *Nucl. Phys. A* **273**, 253 (1976)
9. Daly, P.J., Kleinheinz, P., Broda, R., Stefanini, A.M., Lunardi, S., Backe, H., Richter, L., Willwater, R., Weik, F.: *Z. Phys. A* **288**, 103 (1978)
10. Blomqvist, J., Kleinheinz, P., Broda, R., Daly, P.J.: *Z. Phys.* (to be published)
11. Gromov, K.Ya., Zuber, K., Latuszynski, A., Penev, I., Potempa, A.V., Zelinski, A., Zuk, V.: *Acta Phys. Pol. B* **6**, 421 (1975)
12. Toth, K.S., Newman, E., Bingham, C.R., Rainis, A.E., Schmidt-Ott, W.-D.: *Phys. Rev. C* **11**, 1370 (1975)
13. Backe, H., Richter, L., Willwater, R., Kankeleit, E., Kuphal, E., Nakayama, Y., Martin, B.: *Z. Phys. A* **285**, 159 (1978)

14. Khoo, T.L.: Proceedings of the symposium on High Spin Phenomena in Nuclei. Argonne, 1979 ANL/PHY-79-4, p. 95 (1979)
  15. Hagemann, D.C.J.M., de Voigt, M.J.A., Jansen, J.F.W.: Phys. Lett. **84B**, 301 (1979)
  16. André, S., Genevey, J., Gizon, A., Gizon, J., Jastrzebski, J., Lukasiak, J., Mosynski, M., Preibisz, Z.: Proceedings of the International Conference on Nuclear Behaviour at High Angular Momentum, Strasbourg, p. 59 (1980)
  17. Kleinheinz, P., Ogawa, M., Broda, R., Daly, P.J., Haenni, D., Beuscher, H., Kleinrahm, A.: Z. Phys. A **286**, 27 (1978)
  18. Kownacki, J., Ryde, H., Sergejev, V.O., Sujkowski, Z.: Nucl. Phys. A **196**, 498 (1972)
  19. Schiffer, J.P., True, W.W.: Rev. Mod. Phys. **48**, 191 (1976)
  20. Cates, M., Ball, J.B., Newman, E.: Phys. Rev. **187**, 1682 (1969)
  21. Kisslinger, L.S., Sorenson, R.A.: Rev. Mod. Phys. **35**, 853 (1963)
  22. Ogawa, M., Broda, R., Zell, K., Daly, P.J., Kleinheinz, P.: Phys. Rev. Lett. **41**, 289 (1978)
  23. Björnstad, T., DeGeer, L.-E., Ewan, G.T., Hansen, P.G., Jonsson, B., Kawade, K., Kerek, A., Lauppe, W.-D., Lawin, H., Mattson, S., Sistemich, K.: Phys. Lett. **91B**, 35 (1980)
  24. Blomqvist, J., Borg, S., Kerek, A., Rensfelt, K.-G., Sztarkier, J.: Phys. Scr. **9**, 321 (1974)
  25. Astner, G., Bergström, I., Blomqvist, J., Fant, B., Wikström, K.: Nucl. Phys. A **182**, 219 (1972)
  26. Kleinheinz, P.: Proc. Symp. on High Spin Phenomena in Nuclei. Argonne, 1979. ANL/PHY-79-4, p. 125 (1979)
  27. Lunardi, S.: Proceedings of XVIII<sup>th</sup> Winter School on Nuclear Structure, Bielsko-Biala (1980)
  28. Kleinheinz, P., Lunardi, S., Ogawa, M., Maier, M.R.: Z. Phys. A **284**, 315 (1978)
  29. Kleinheinz, P., Maier, M.R., Diamond, R.M., Stephens, F.S., Sheline, R.K.: Phys. Lett. **53B**, 442 (1975)
  30. Bohr, A., Mottelson, B.: Nuclear structure. Vol. II, p. 564. New York: W.A. Benjamin 1975
  31. Häusser, O., Taras, P., Trautmann, W., Ward, D., Alexander, T.K., Andrews, H.R., Haas, B., Horn, D.: Phys. Rev. Lett. **42**, 1451 (1979)
  32. Lunardi, S., Ogawa, M., Maier, M., Kleinheinz, P.: Proc. Symp. on High Spin Phenomena in Nuclei. Argonne, 1979. ANL/PHY-79-4, p. 393 (1979)
  33. Fromm, W.D., Funke, L., Schilling, K.D.: Phys. Scr. **12**, 91 (1975)
  34. Lunardi, S., Ogawa, M., Backe, H., Piiparinen, M., Nagai, Y., Kleinheinz, P.: Proc. Symp. on High Spin Phenomena in Nuclei. Argonne, 1979. ANL/PHY-79-4, p. 403 (1979)
  35. Piiparinen, M., Lunardi, S., Kleinheinz, P., Backe, H., Blomqvist, J.: Z. Phys. A **290**, 337 (1979). (Our recent conversion electron measurements confirm the 839 keV  $E1$  multipolarity of [14].)
- P.J. Daly  
 Institut für Kernphysik  
 Kernforschungsanlage Jülich GmbH  
 Postfach 1913  
 D-5170 Jülich 1  
 Federal Republic of Germany  
 and  
 Chemistry Department  
 Purdue University  
 W. Lafayette, IN 47907  
 USA
- P. Kleinheinz  
 R. Broda  
 S. Lunardi  
 Institut für Kernphysik  
 Kernforschungsanlage Jülich GmbH  
 Postfach 1913  
 D-5170 Jülich 1  
 Federal Republic of Germany
- H. Backe  
 Institut für Kernphysik  
 Technische Hochschule Darmstadt  
 Schloßgartenstraße 9  
 D-6100 Darmstadt  
 Federal Republic of Germany
- J. Blomqvist  
 Research Institute of Physics  
 S-10405 Stockholm 50  
 Sweden